TRITA-EPP-86-09

TESTING A VERY GOOD MICROWAVE INTERFEROMETER

Nils Brenning

October 1986

Department of Plasma Physics
The Royal Institute of Technology
S-100 44 Stockholm, Sweden

TESTING A VERY GOOD MICROWAVE INTERFEROMETER

Nils Brenning
The Royal Institute of Technology, Dept of Plasma Physics
S-100 44 Stockholm, Sweden

Abstract

A 4 mm microwave interferometer is described, together with a working system for numerical evaluation of the recorded signals. The interferometer signals are processed in a computer to provide immediate display of the plasma column density. The numerical evaluation makes it possible to eliminate the influence of also rather large imperfections in the components, and to take into account large and rapid variations in the strength of the transmitted microwave signal. The limits of performance of the system are tested in a pulsed plasma source. Column plasma densities are measured from 10^{15} m^{-2} to $3 \cdot 10^{18}$ m^{-2}, corresponding to phase swings from less than one degree up to several times 360^{o}. The upper limit corresponds to densities approaching the cutoff density, $6 \cdot 10^{19}$ m^{-3}, where reflection and refraction of the transmitted beam become severe. Measurements were possible even when the power in the transmitted branch was reduced (due to the plasma) by more than a factor 30, and when the transmitted power varied as rapidly as a factor 4 in 200 ns.

1. Introduction

This paper describes the operating and testing of a microwave interferometer for plasma density measurements. The interferometer is a development of the interferometers described by Hotston and Seidl (1965), and Lindberg and Eriksson (1982). It is described by Brenning (1984), herein referred to as paper I). It was constructed with the aim to make measurements possible also when the microwave power, in the branch that passes through the plasma, is strongly reduced and varies rapidly in time. It was also intended to computerize the evaluation so that results could be obtained at the touch of a button, for phase swings from a few degrees up to the upper limit, usually several times 360^{o}, at which cutoff makes microwave interferometry impossible.

The numerical evaluation of the interferometer signals is described in Section 2. The testing of the interferometer system in a pulsed plasma source is reported in Section 3, and some suitable error checks and messages, which facilitate the use of the interferometer, are described in the Appendix.

2. Evaluation of the recorded signals

We will here limit the discussion to the numerical evaluation of the signals. The reader is referred to Paper I for the construction of the microwave circuit, the derivation of equations and the initial setting of phase angles.

The interferometer circuit is shown in Fig. 1. It has two branches, the reference (or R-) branch, and the transmitted (or T-) branch. The microwave signals in the two branches are added with suitable phase shifts and measured in two detectors, labelled 1 and 2. The quantities that are needed for the evaluation are summarized in Table 1. They are: (1) the detector signals U_{1R} and U_{2R} in the R branch with the T branch cut

off, (2) the signals U_{1TO} and U_{2TO} in the T branch with the R branch cut off, and (3) the signals U_{10} and U_{20} with both branches open, but without plasma. The recordings with plasma are called $U_1(N)$ and $U_2(N)$, where N is the number of the timepoint in the recording.

The calculation of the T-branch phase angle φ from measured quantities is illustrated in Fig. 2a, which is taken from Paper I. The indices on the normalized electric field phasors in Fig. 2a have the same meaning as they have for the detector signals of Table 1. We here assume that the detector response is quadratic; otherwise, one can correct the detectors for the deviation from quadratic detector response, and then proceed as with quadratic detectors. The method of correction is described by Lindberg and Eriksson (1982).

For each timepoint N of the recording, an angle φ lying between 0 and 360^{o} is obtained by the successive solution of the Equations (1) to (6):

$$A = \left[\frac{u_{1R}}{u_{1TO}} + \frac{u_{2R}}{u_{2TO}} + \frac{u_1(N)}{u_{1TO}} - \frac{u_2(N)}{u_{2TO}}\right] x \left\{2\left(\frac{u_1(N)}{u_{1TO}}\,\frac{u_{1R}}{u_{1TO}} + \frac{u_{2R}}{u_{2TO}}\right)^{1/2}\right\}^{-1} \qquad (1)$$

$$\alpha = \tan^{-1}\left(\frac{u_{2R}/u_{2TO}}{u_{1R}/u_{1TO}}\right)^{1/2} \qquad (2)$$

$$\beta = \cos^{-1} A \qquad (3)$$

$$x - x_o = \left(\frac{u_1(N)}{u_{1TO}}\right)^{1/2} \cos\beta - \left(\frac{u_{1R}}{u_{1TO}}\right)^{1/2} \cos\alpha \qquad (4)$$

$$y - y_o = \left(\frac{u_1(N)}{u_{1TO}}\right)^{1/2} \sin\beta - \left(\frac{u_{1R}}{u_{1TO}}\right)^{1/2} \sin\alpha \qquad (5)$$

and

$$\varphi = \tan^{-1}\left(\frac{y-y_o}{x-x_o}\right) \begin{cases} +90 & \text{if } (x-x_o) \geq 1 \\ +270^{o} & \text{if } (x-x_o) < 1 \end{cases} \qquad (6)$$

For high plasma densities, where the phase swing is large, a multiple of 360° may have to be added to φ. The correct multiple is obtained by following the plasma density increase from (or decrease to) zero.

The plasma column density is given by the phase swing from the angle φ_o obtained in the absence of plasma:

$$n_e(x,t)dx = (\varphi-\varphi_o)\frac{\lambda_o n_c}{\pi} \qquad (7)$$

where λ_o is the vacuum wavelength,
and $n_c = 4\pi^2 m_e(\mu_o e^2 \lambda_o^2)^{-1}$ is the cut-off density. Eq. (7) is strictly valid only when $n_e \ll n_c$. For electron densities approaching the cut-off density, it tends to underestimate the electron density by approximately the factor $(n_e/2n_c)/(1-\sqrt{1-n_e/n_c})$. (This factor is immediately obtained from Eqs (1) and (2) of Paper I.) For $n_e < 0.5 n_c$, the error is below 20%.

The power attenuation in the T branch, finally, is given by

$$P/P_o = (x-x_o)^2 + (y-y_o)^2 \qquad (8)$$

A block diagram for computer-controlled recording and evaluating the interferometer signals is shown in Fig.3. Some practical aspects of the evaluation are discussed in the Appendix.

3. Testing the interferometer

The interferometer was tested with a pulsed plasma source, which has been described elsewhere (Brenning et al. 1981). The plasma is produced by a discharge in a conical theta pinch, and shot along a guiding magnetic field to the interaction space, where the interferometer is situated. The plasma density can be varied several orders of magnitude by changing the parameters of the plasma gun.

The limits of performance of the interferometer are of two types, (1) the high-density limit, where reflection and refraction reduce the transmitted power too much, and (2) the low--density limit, where the phase swing one tries to measure competes with noise and other error sources, e.g. vibrations of the microwave horns and drift of the amplifiers and the microwave source.

For precision measurements of low densities it is essential that the signal levels without plasma (U_{10} and U_{20}) are taken as close in time to the actual measurements as possible. For example, a displacement of the microwave horns with 1/100 mm corresponds to a phase shift of 1 degree, or a column density of $1.7 \cdot 10^{15}$ m^{-2}.

Fig. 4 shows examples of measurements close to the low-density limit. To the left are shown "zero lines" without plasma in the T branch; to the right, measurements with plasma. The upper panels show one-shot recordings, and the lower panels averages over 10 shots. The resolution in a noise-free surrounding would be around $2 \cdot 10^{15}$ m^{-2} for single shots and $5 \cdot 10^{14}$ m^{-2} for 10-shot averages (corresponding to a 1/4 degree phase swing). Due to noise associated with the discharge of our plasma source, our actual resolution was not quite so good. We achieved around 10^{16} m^{-2} for single shots, and $2 \cdot 10^{15}$ m^{-2} for averages over 10 shots (right-hand panels of Fig. 4).

When averages are made , they shall be averages of calculated densities. It is <u>not</u> suitable to average detector signals first, and then calculate the density. At low densities, the latter procedure is less efficient in eliminating vibrations of the microwave horns, low-frequency noise and long-term drifts. At high densities, where the power in the transmitted beam can be strongly reduced, it could easily give completely erroneous results.

One example of measurements close to the high density limit is shown in Fig. 5. To the left are shown the unprocessed signals

from the two detectors, which nicely illustrate the phase shift between them; the lower detector is leading with 90^{o} when the density increases and lagging with 90^{o} when it decreases again.

The plasma is in the form of a flat slab, with a thickness of approximately 0.1 m, which is shot perpendicular to the line of sight of the interferometer. The microwave horns are 1.2 m apart, and carefully focussed on each other. The high-velocity plasma stream gives a rapidly varying refraction of the beam, and also some reflection. As a result, the power in the transmitted beam varies rapidly, as shown in the right-hand panels of Fig. 5. The strongest reduction (a factor of 10) and the most rapid fluctuations (a factor 4 over 200 ns) occur around the density maximum. They are shown with extended time scale in the lower right-hand panel.

The calculated column density from the same shot is shown in Fig.6. It is not filtered in any way. The smoothness of this curve, compared to the rapid fluctuations in the power levels of the transmitted signals, illustrates how well the interferometer can distinguish between phase shifts and density variations. It also keeps track correctly of the turnings of 360^{o}; measurements with slower time sweeps show that the density decays back to zero as it should.

The highest plasma column density we were able to measure was $3 \cdot 10^{18}$ m^{-2}, which in our plasma source corresponds to a peak density just below $3 \cdot 10^{19}$ m^{-3} (approximately half the cut-off density). The power in the transmitted branch was for these densities reduced by typically a factor 30, which made necessary rather frequent and careful calibration of the interferometer, as described in the Appendix.

Acknowledgements

I want to thank Drs I. Axnäs and L. Lindberg for many stimulating discussions. This work has been financed by the Swedish Natural Science Research Council.

APPENDIX

Fig. 3 shows a block diagram for the recording and evaluation of the interferometer signals. When a recording is to be made, the user is first offered an opportunity to calibrate the interferometer, i.e., read new values of U_{1R}, U_{2R}, U_{1TO} and U_{2TO}. It is preferable to measure U_{1TO} and U_{2TO} before U_{1R} and U_{2R}, since one then does not have to touch the attenuators ATT3 And ATT4 in the R branch (Fig.1) after measuring the transmission in that branch; a very accurate measurement of the R branch power is essential if one wants to measure high plasma densities, where the T branch transmission becomes strongly reduced.

After this calibration a recording with a pulsed plasma is made, giving $U_1(N)$ and $U_2(N)$, where N is the number of the timepoint. In our case it was possible to trigger the recording well before the plasma density started to increase. The detector signals without plasma (U_{10} and U_{20}) could therefore be obtained individually for each shot from the time before plasma arrival. As discussed in Section 3, this is essential for precision measurement of low densities. The initial phase angle φ_o is then obtained from Eqs (1)-(6), using U_{10} and U_{20} instead of $U_1(N)$ and $U_2(N)$.

The plasma column density $\int n_e(x,t)dx$, and the T branch power attenuation, are then calculated as shown in the block diagram of Fig.3, by successively solving Eqs (1)-(8) for each timepoint N. There are three openings for error messages in this calculation:

Error message 1 is displayed in case the quantity A (given by Eq. (1)) is an invalid argument to the arccos function of Eq. (3). This happens if the measured values $U_1(N)$ and $U_2(N)$ at some timepoint correspond to phasor lengths E_1 end E_2 (Fig. 2a) which together are shorter than the distance AB. In

our case this occurred under either of two circumstances: first if the recording as triggered simultaneously as the main discharge of the plasma source, which added considerable noise to the detector signals; second, if the power in the T branch was so large that the situation with the angle $\beta \approx 0$ shown in Fig. 2b could arise. In this case, also a small noise level on $U_1(N)$ and $U_2(N)$ could give invalid arguments to the arccos function. The search for the type of error is simplified by error message 1, which gives the time of the error, and value of β for the last previous timepoint.

Error message 2 is displayed if the angle β at any timepoint is below 5 degrees. The reason for this error message is that a given pair of E_1 and E_2 in Fig. 2a in principle also can be caused by mirroring in the x-axis. To exclude this ambiguity, one has to set the power in the T branch so low that the phasor tip always corresponds to positive y. However, for low plasma densities (where the highest phase shift resolution is desired) one may want to operate with the T branch power at maximum and with an initial phasor location with $\underline{E}_T$ approximately straight up in Fig. 2a. The check that β is always greater than 5 degrees (which is an arbritarily choosen value) ensures that the measurement still is unambiguous.

Error message 3 is displayed if the phase charge $\Delta\varphi$ between two consecutive timepoints is found to be larger than $\pm\ 30^o$ (again an arbritarily choosen value) which makes the counting of multiples of 360^o somewhat uncertain. After displaying this error message, the plasma column density is put equal to zero for the remaining timepoints. The power attenuation P/Po, however, can still be correctly obtained from Eqs (1)-(5) and Eq. (8). It is therefore calculated for the whole time period of recording. This procedure allows display of the plasma density increase up to cut-off, which in our case was the usual reason for this kind of error message: with the T branch power approximately zero, noise in the detectors makes the phasor tips apparently move about in a random fashion around the

position (x_o, y_o) of Fig. 2a, quickly giving phase shifts greater than $\pm$ 30 degrees.

References

Brenning, N. (1984), An Improved Microwave Interferometer Technique for Plasma Density Measurements, J. Phys. E: Sci. Instrum. 17, 1018-1023

Brenning, N., Lindberg, L., and Eriksson, A. (1981), Energization of Electrons in a Plasma Beam Entering a Curved Magnetic Field, Plasma Physics, 23, 559-574

Hotston, E. and Seidl, M. (1965), A Microwave Interferometer for the Measurement of Small Phase Angles, J. Sci. Instrum., 42, 225-230.

Lindberg, L. and Eriksson, A., (1982), Optimum Design of a Microwave Interferometer for Plasma Density Measurements, J. Phys. E: Sci. Instrum. 15, 548-554

	With R branch?	With T branch?	With plasma?
U_{1R}	yes	no	no
U_{2R}	yes	no	no
U_{1TO}	no	yes	no
U_{2TO}	no	yes	no
U_{1O}	yes	yes	no
U_{2O}	yes	yes	no
$U_1(N)$	yes	yes	yes
$U_2(N)$	yes	yes	yes

Table 1. The quantities needed for evaluating the plasma density. The indices 1 and 2 indicate the number of the detector. N is the number of the timepoint in a time-dependent recording with plasma.

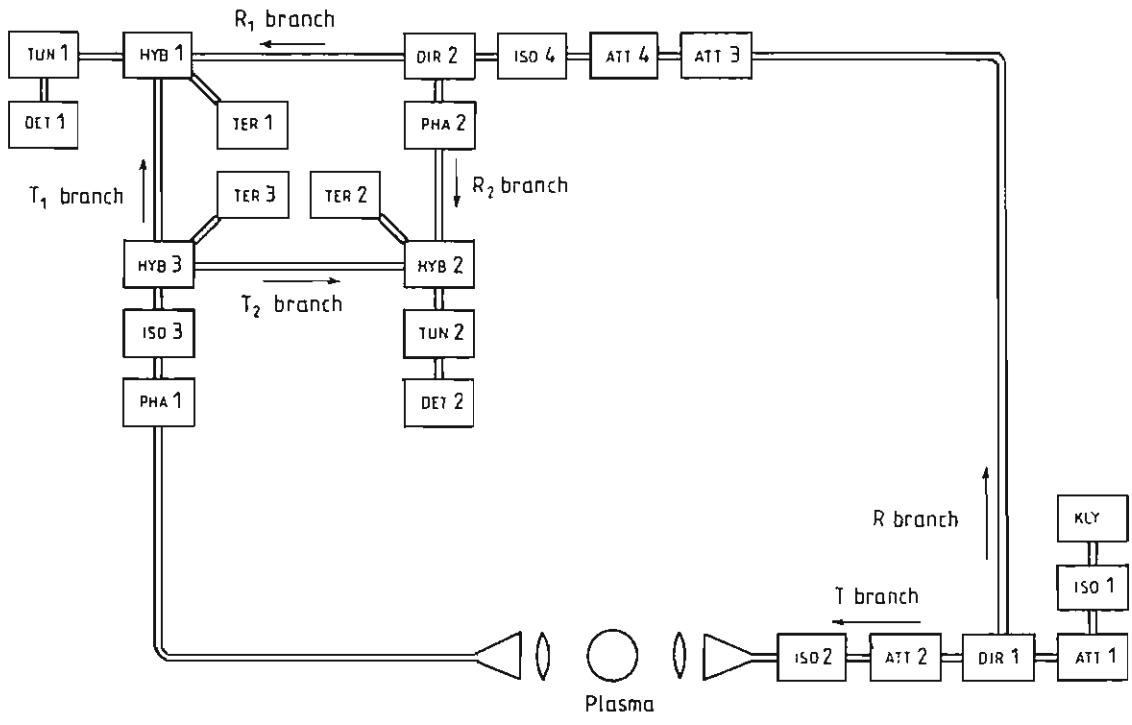

Figure 1. The interferometer bridge circuit. Notations: ATT = attenuator, DET = directional coupler, HYB = hybrid ("Magic T" or hybrid ring), ISO = isolator, KLY = klystron, PHA = variable phase shifter, TER = terminating load, and TUN = tuner. (From Brenning, 1984)

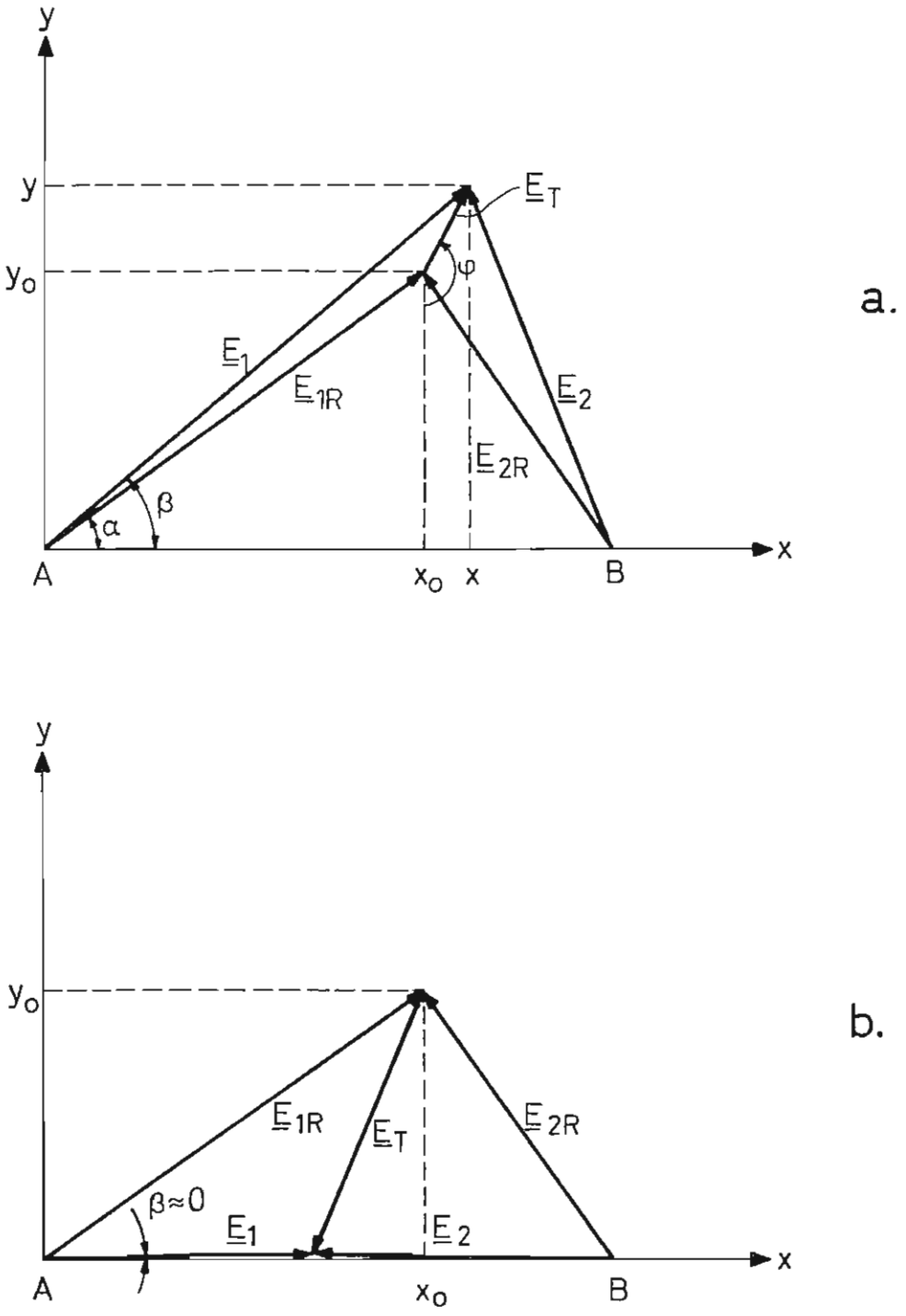

Figure 2. (a): Calculation of the phase angle φ of the T branch
(b): A situation where noise easily can give rise to invalid arguments in the $\cos^{-1}$ function of Eq.(3)

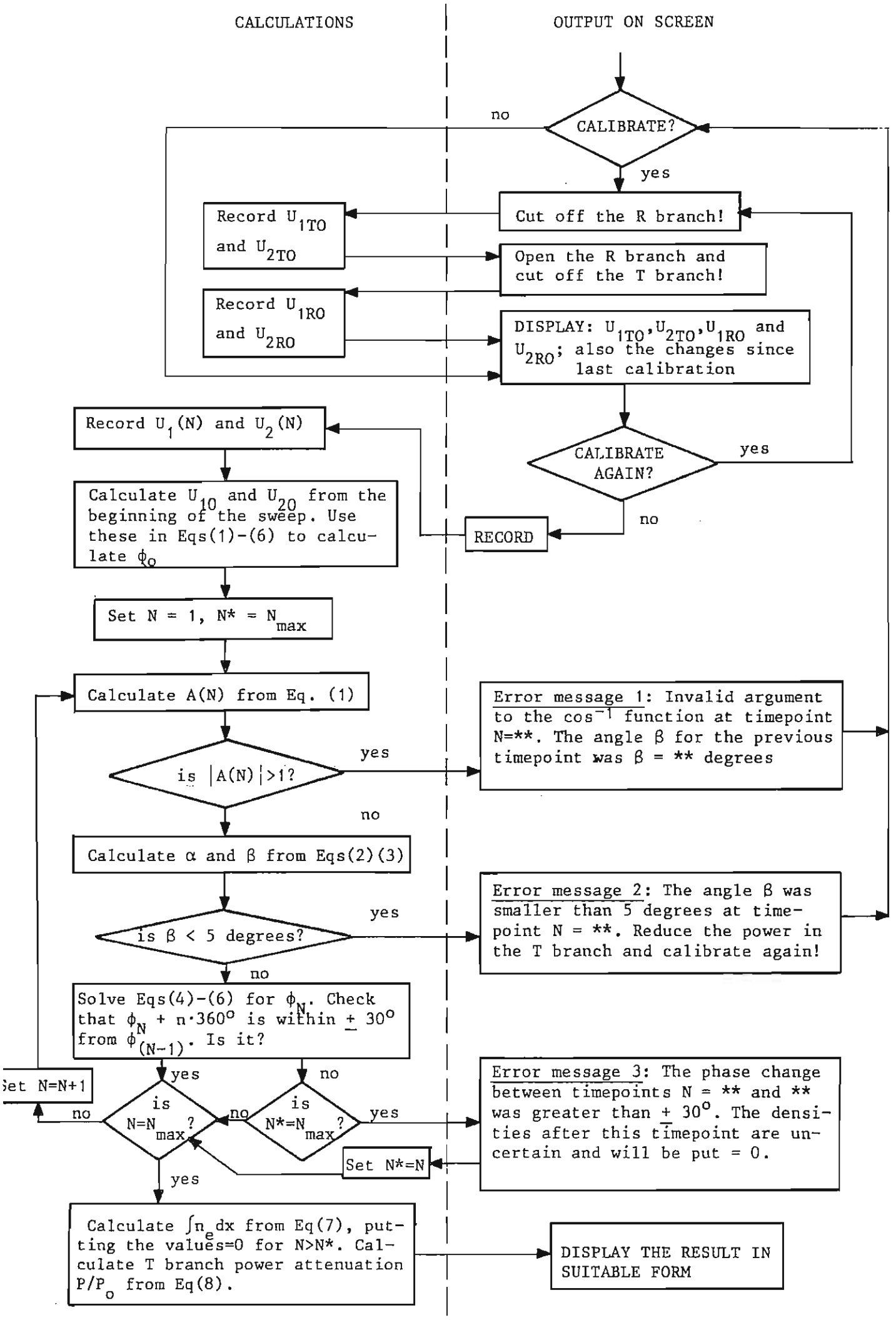

Figure 3. A block diagram for the numerical evaluation of the detector signals

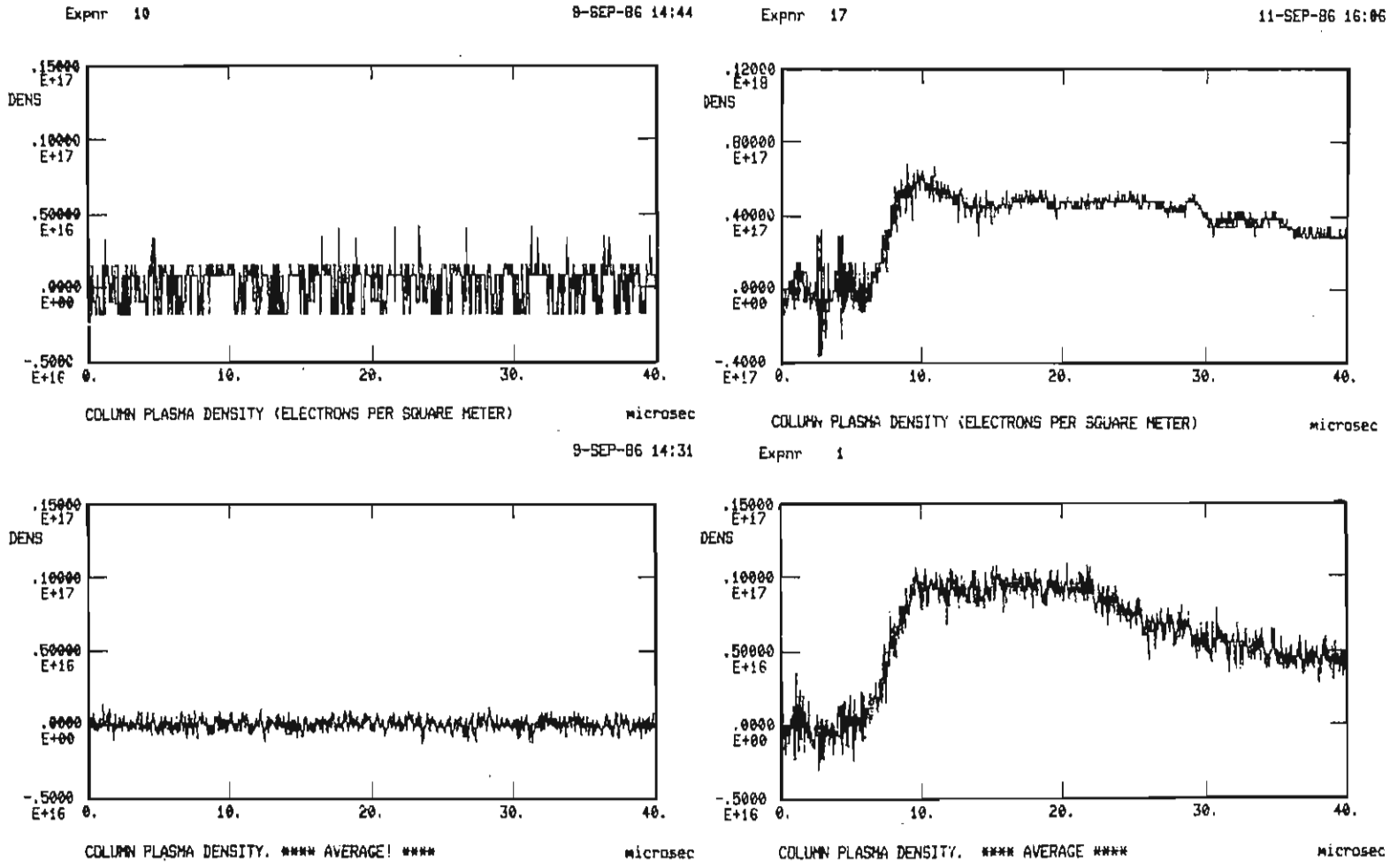

Figure 4. Measurements at low densities. The left-hand panels show the "zero level" obtained without plasma in the T branch; the right-hand panels are recordings with plasma. The two upper panels are singel shot recordings, while the lower panels are averages over ten shots. A phase swing of 1 degree corresponds to $1.65 \cdot 10^{15}$ m^{-3}.

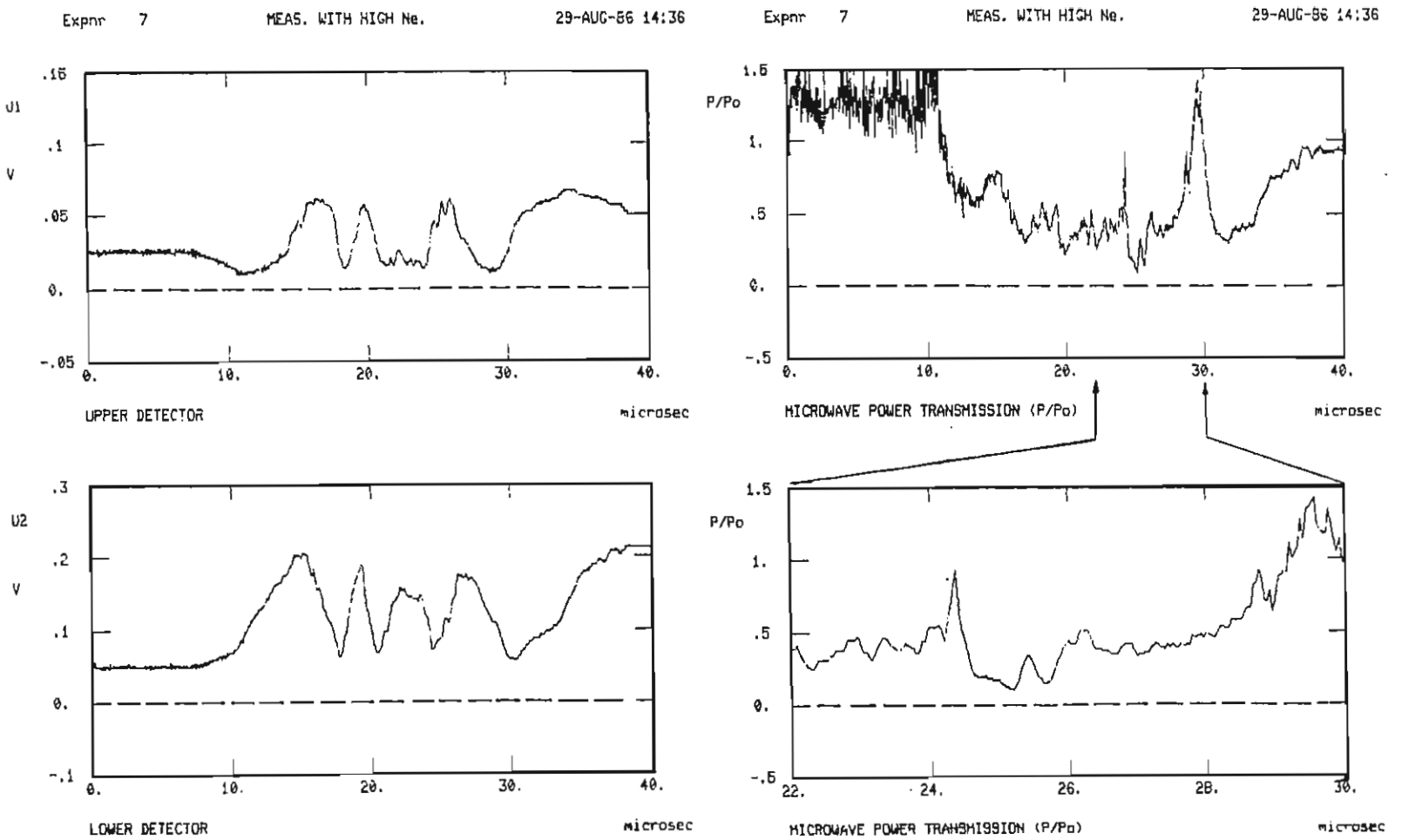

Figure 5. Measurements at high densities. The left-hand panels show the two detector signals and the right-hand panel the (calculated) power in the beam that passes through the plasma. The lower right-hand panel shows the near-cutoff, which occurs at maximum plasma density, on an expanded time scale.

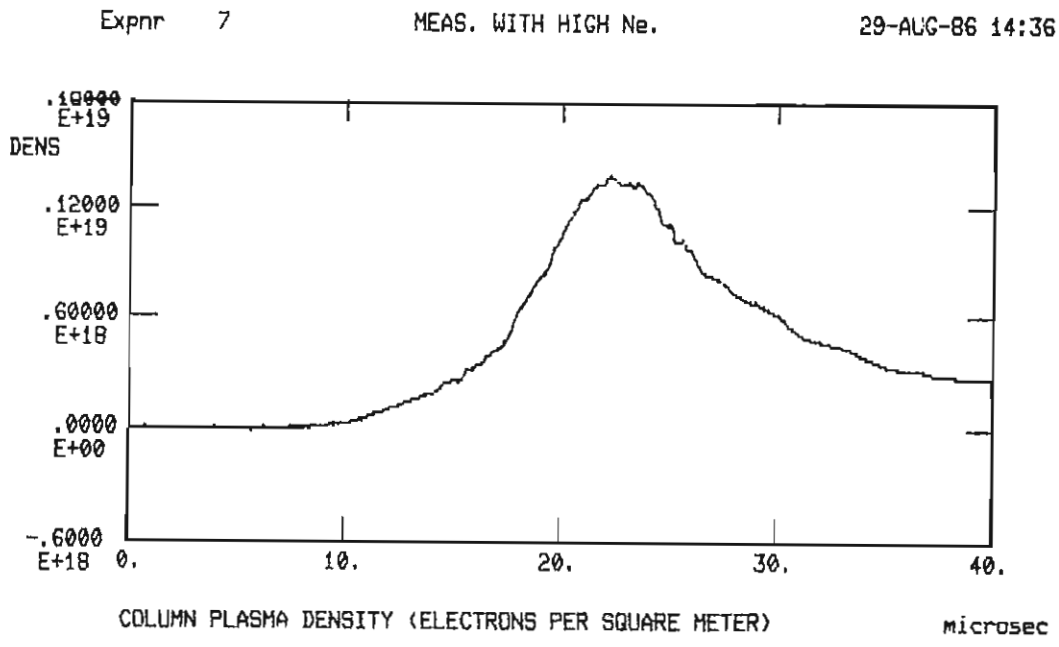

Figure 6. The density calculated from the detector signals of Fig. 5. The curve has not been filtered or smoothed in any way.

TRITA-EPP-86-09 ISSN 0348-7539

The Royal Institute of Technology, Department of Plasma Physics
S-100 44 Stockholm, Sweden

TESTING A VERY GOOD MICROWAVE INTERFEROMETER

Nils Brenning
September 1986, 19 pp. incl. ill., in English

A 4 mm microwave interferometer is described, together with a working system for numerical evaluation of the recorded signals. The interferometer signals are processed in a computer to provide immediate display of the plasma column density. The numerical evaluation makes it possible to eliminate the influence of also rather large imperfections in the components, and to take into account large and rapid variations in the strength of the transmitted microwave signal. The limits of performance of the system are tested in a pulsed plasma source. Column plasma densities are measured from 10^{15} m^{-2} to $3 \cdot 10^{18}$ m^{-2}, corresponding to phase swings from less than one degree up to several times 360^{o}. The upper limit corresponds to densities approaching the cutoff density, $6 \cdot 10^{19}$ m^{-3}, where reflection and refraction of the transmitted beam becomes severe. Measurements were possible even when the power in the transmitted branch was reduced (due to the plasma) by more than a factor 30, or when that power varied more as rapidly as a factor 4 in 200 ns.

Key words: Microwave interferometry, Plasma diagnostics, Plasma density measurements